1 Sergey A. Karpov [1,2,*], Albert Reñé [3], Andrey E. Vishnyakov [2], Kensuke Seto [4,5], Elisabet Alacid [3,6],

2 Aurora Paloheimo [7], Maiko Kagami [4], Anke Kremp [8], Esther Garcés [3]

3

Parasitoid chytridiomycete *Ericiomyces syringoforeus* gen. et sp. nov. has unique cellular

structures to infect the host

6

7

8 [1] Zoological Institute of Russian Academy of Sciences, Universitetskaya nab. 1, St.

9 Petersburg, 199034 Russia.

10 [2] Department of Invertebrate Zoology, Biological Faculty, St. Petersburg State University,

11 Universitetskaya nab. 7/9, St. Petersburg, 199034 Russia

12 [3] Departament de Biologia Marina i Oceanografia. Institut de Ciències del Mar (CSIC). Passeig

13 Marítim de la Barceloneta, 37-49 08003 Barcelona, Catalonia (Spain)

14 [4] Yokohama National University, Graduate school of Environment and Information Sciences,

15 Tokiwadai 79-7, Hodogayaku, Yokohama, 240-8501, Kanagawa, Japan

16 [5] Current address: Department of Ecology and Evolutionary Biology, University of Michigan,

17 1105 North University, Ann Arbor, MI 48109, USA.

18 [6] Current address: Department of Zoology, University of Oxford, 11a Mansfield Rd, Oxford, OX1

19 3SZ (UK)

20 [7] Finnish Environment Institute, Marine Research Centre, Latokartanonkaari 11, 00790 Helsinki,

21 Finland

22 [8] Leibniz Institute for Baltic Sea Research Warnemünde, Department of Biological

23 Oceanography, Seestraße 15, 18119 Rostock, Germany

24

25 *** Corresponding author e-mail: sakarpov4@gmail.com**

26 **ORCID: 0000-0002-1509-1908**

27

28

29

30

31

32

33

34

35

36

37

38 **Abstract**

39 Many fungi have been identified as pathogens of marine algae. Among them, Chytridiomycota

40 have been revealed as relatively highly abundant, but much of the diversity known within these

41 groups is almost entirely based on environmental sequencing data. Here, we present a novel

42 chytridiomycete genus and species, characterized by light microscopical observations,

43 ultrastructure, and molecular phylogenetic analysis of the parasitic chytrid of brackish-water

44 dinoflagellate *Kryptoperidinium foliaceum* from the Baltic Sea. Phylogenetic analysis of rDNA

45 sequences and the ultrastructure of the strain reveals that it represents a new family in the

46 order Rhizophydiales. *Ericiomyces syringoforeus* gen. et sp. nov. is a parasitoid with a life cycle

47 composed by zoospores, which attach to the host, encyst and produce a rhizoidal system

48 (haustorium). Unlike typical Rhizophydiales chytrids, sporangium develops as a lateral

49 outgrowth of the encysted zoospore. The ultrastructural study revealed at least two unique

50 traits: the syringe-like organelle in the cyst, which supposed to paralyze the host, and funnel-

51 shaped structure anchoring sporangium in the host wall. Sporangium matures and produces

52 new zoospores within three days. Multiple infection is common and then the life-cycle is one-

53 two days shorter compared to the duration when a single infection occurred. Cross-infection

54 experiments showed that *E. syringoforeus* could only infect dinoflagellates, being *K. foliaceum*

55 highly susceptible to infection by the chytrid parasitoid. The effects of some fungal epidemics

56 on populations of *Kryptoperidinium* are discussed.

57

58 **Keywords:** brackish-water, Rhizophydiales, Ericiomycetaceae, dinoflagellate, ultrastructure,

59 molecular phylogeny

60

61

62

63

64

65

66

67

68

69 **Introduction**

70 Traditional studies utilizing microscopy and culture isolation have demonstrated that marine

71 fungi are relatively species-poor, predominantly Dikarya, and localized to coastal habitats. To

72 date, only a relatively small number of described fungi, approximately 1,100 species, have been

73 retrieved exclusively from the marine environment (Amend et al. 2019). Using high-throughput

74 diversity tag sequencing from both DNA and RNA templates counts, Richards et al. (2015) have

75 studied the diversity and abundance of fungi in marine samples from European near-shore

76 sites. In these samples they have shown unexpectedly high abundance of Chytridiomycota,

77 accounting for nearly 60% of all fungal sequences (Richards et al. 2015). Picard (2017) also

78 noted that the diversity of marine fungi was highest in sand flats and wetland sediments,

79 though benthic sediments harboured the highest proportion of novel sequences. Particularly

80 notable were a large number of species belonging to "early diverging lineages" such as the

81 Chytridiomycota (chytrids), which tend to dominate nearshore and sediment samples (Le Calvez

82 et al. 2009, Richards et al. 2012, 2015, Comeau 2016). Much of the diversity known within these

83 groups is almost entirely based on environmental sequencing data (Amend et al. 2019). Thus,

84 the environmental sequences demonstrate the existence of a great diversity of zoosporic fungi

85 in the sea, but the studies of the putative species in the lab, culturing them to study their

86 morphology, are lacking. At the same time, classical investigations are really needed, as they

87 often demonstrate exclusively unusual morphological diversity describing new phenomena in

88 fungal cell structure, which leads to new insights on the diversity and early evolution of fungi

89 (Karpov et al. 2018).

90 Chytrids are ubiquitous in aquatic, predominantly freshwater, environments and are largely

91 recognized as phytoplankton parasites (Frenken et al. 2017, Gleason et al. 2015, Kagami et al.

92 2007, Scholz et al. 2016). At least six chytrid species infect freshwater dinophytes (Dangeard

93 1888, Canter 1968, Canter and Heaney 1984, Alster and Zohary 2007, Leshem et al. 2016).

94 However, fewer chytrid species are known from marine environments (Jones et al. 2015, 2019,

95 Powell 2016, Garvetto et al. 2019), and only one species capable of parasitizing marine

96   dinoflagellates is currently known, *Dinomyces arenysensis,* which infects the toxic dinoflagellate

97   *Alexandrium minutum* (Lepelletier et al. 2014b).

98   Here, we present a novel chytridiomycete genus and species, characterized by light

99   microscopical observations, ultrastructure, and molecular phylogenetic analysis of a strain

100 isolated from brackish-marine[1] water samples of the coastal Northern Baltic Sea that parasitizes

101 the dinoflagellate *Kryptoperidinium foliaceum*, and represents the first species infecting

102 dinoflagellates in brackish waters. Phylogenetic analysis of rDNA sequences and the

103 ultrastructure of this strain supports the representation of a new family in the order

104 Rhizophydiales.

105

106 **Materials and Methods**

107 **Sampling.** The sampling was carried out on Kökar, and island belonging to the Åland

108 Archipelago (SW coast of Finland) in the northern Baltic Sea, in June 2016 as described in Alacid

109 et al. (in press). The sampling point was located in a shallow coastal embayment (2–3 m deep).

110 As typical for this area, salinities of 6–7‰ prevail and water temperatures can reach up to 24 ^{o}C

111 during summer (Kremp et al. 2009, Hakanen et al. 2012). Two water samples, pre-sieved

112 through a 76-μm mesh, were collected from a small boat at the sampling point: (1) a surface

113 water sample, which was filled from a jug directly into a 5 L plastic bottle; and (2) a net tow

114 sample with a mesh size of 10 μm, which was obtained from integrating water slowly through

115 the whole water column. The net sample was poured into a 200-ml polystyrene culture flask.

116 Information about the sampling strategy and host/phytoplankton community composition is

117 detailed in Alacid et al. in press.

118 **Detection, isolation, and cultivation of the zoosporic parasites.** From 2 to 5 L of water from

119 the surface samples were concentrated using a 10 μm mesh, and aliquots were distributed into

120 separate wells of polystyrene 12-well tissue culture plates. These concentrated surface samples

121 and net samples were incubated for several days at 20 ^{o}C, and a photoperiod of 12:12

122 (light:dark) and observed daily with an inverted microscope (Leica DMI3000B) to detect

123 infection by parasitoids. After a few days, chytrids infecting *Kryptoperidinium foliaceum* in these

124 concentrated isolates were observed. Infected cells were manually isolated with glass capillary

---

[1] Restrictly speaking most of the described marine chytrids occur, in fact, in brackish waters
(0.5-30 psu) (e.g. Lepelletier et al. 2014b, Letcher et al. 2015). Below we use "brackish" rather
than "marine".

125 micropipettes and individually placed in 96-well tissue culture plates. Cells of *K. foliaceum*

126 originating from the studied area strain KFF 1003 from the culture collection of the Finnish

127 Environment Institute (SYKE), grown in F/2 –Si local seawater based medium (salinity 6‰),

128 were added to the well-plates to serve as host, and incubated in culturing chambers at 21 ^{o}C,

129 14:10 (light:dark period). Once infections were propagated in the well-plate, a small volume of

130 the co-culture was transferred to a new well and new healthy host cells were provided. This

131 procedure was done twice a week throughout three years. Unfortunately, in September 2019,

132 the cultured strain E4 was lost.

133 **Microscopy.** Sub-samples of cultured cells infected by the chytrid were taken at different stages

134 of the infection development in order to characterize the morphology and ultrastructure of the

135 different life-cycle stages of the chytrid. 2 mL of live samples were transferred to settling

136 chambers and observed with a phase-contrast Leica DM-IRB inverted microscope (Leica

137 Microsystems, Wetzlar, Germany) connected to a ProgRes C10 (JENOPTIK Laser, Optik, Systeme

138 GmbH, Jena, Germany) digital camera and a Zeiss Axioplan microscope equipped with a color

139 MRm Axiocam camera. For scanning electron microscopy (SEM), 5 mL of chytrid culture were

140 fixed with 10% formaldehyde (v:v) and filtered by gravity on an 8 μm pore size polycarbonate

141 filter. Samples were then washed in filtered seawater for 15 min and in distilled water for 15

142 min. Subsequent dehydration was carried out in a 25, 50, 75, 90, 96, and 100% ethanol series

143 for ca. 10 min. The final step of 100% ethanol was repeated twice. The filters were critical-point

144 dried and mounted on stubs, sputter-coated with gold-palladium and examined under a

145 HITACHI S-3500N scanning electron microscope (Hitachi High Technologies Corp., Tokyo, Japan)

146 at the Servei de Microscopia Electrònica (ICM-CSIC).

147 For transmission electron microscopy (TEM) the infected cultures were fixed after

148 centrifugation at a final concentration of 2% of glutaraldehyde prepared in the culture medium

149 and stored at 4 ^{o}C for 2 hours. After washing in the culture medium, the pellet was fixed in 1%

150 osmium tetroxide solution at 4 ^{o}C for 1 hour. The pellet was washed twice in the culture

151 medium and embedded in Spurr's resin after dehydration in ethanol and propylene oxide.

152 Serial ultrathin sections were obtained using a diamond knife on an Ultracut microtome and

153 double stained before observation with a JEOL TEM JEM-1400.

154

155 **Sequencing and phylogenetic analysis.** Mature sporangia were manually isolated using a glass

156 micropipette, transferred to successive drops of autoclaved 6‰ seawater and placed into 200

157   μL PCR tubes. PCR tubes were subjected to freeze-thaw rounds and stored at -80 ^{o}C until

158   processed. To amplify 28S rDNA, we used the primer pair D1R (Scholin et al. 1994) and D3B

159   (Hansen et al. 2000) using a 25 μL PCR mix containing 1X Buffer, 1.5 mM MgCl$_2$, 0.2 mM of each

160   dNTP, 0.4 μM of each primer and 2 U of Taq Platinum DNA polymerase (Invitrogen). PCR

161   conditions were as follows: initial denaturation for 5 min at 95 ^{o}C, 40 cycles of 20 s at 95 ^{o}C, 30

162   s at 55 ^{o}C, and 1 min at 72 ^{o}C, followed by a final extension step for 7 min at 72 ^{o}C. For ITS

163   region, the same PCR mix was used with primers ITS1 and ITS4 (White et al. 1990) and the same

164   PCR conditions as before. Finally, DNA from the culture, also including the host genetic

165   material, was obtained. 15 mL of culture were pelleted with a first centrifugation at 3,000 rpm x

166   15 min, the supernatant was removed, and the pellet was transferred to a 1.5 mL tube. It was

167   centrifuged at 10,000 rpm x 5 min and its DNA was extracted with DNeasy Blood & Tissue kit

168   (Qiagen) following the manufacturer's instructions. One μL of DNA was used as template to

169   obtain the partial 18S rDNA sequence under the same PCR conditions as before, using the

170   specific primers Crypto2-2F and AU4v2 (Lazarus and James 2015). Purification and sequencing

171   were carried out by an external service (Genoscreen, France), using forward and reverse

172   primers for all primer pairs and a 3730XL DNA sequencer. The sequences obtained were aligned

173   with a selection of sequences covering the diversity of Rhizophydiales, as well as

174   representatives of other Chytridiomycota groups obtained from GenBank, using online version

175   of MAFFT (Katoh et al. 2019) under L-INS-i option. Subsequently, the alignments were trimmed

176   using trimAl (Capella-Gutiérrez et al. 2009) under the gappyout option. The ITS1 and ITS2

177   regions were excluded from the alignment manually with BioEdit v 7.0.5 (Hall, 1999). Resulting

178   alignments had 5037 positions for concatenated 18S+5.8S+28S rDNA (Chytridiomycota

179   dataset), 1521 positions for 18S rDNA, 849 positions for 28S rDNA, and 1008 positions for

180   concatenated 5.8S + 28S rDNA (Rhizophydiales datasets). GenBank accession numbers of all

181   sequences used are listed in Table S1. Phylogenetic relationships were determined as described

182   in Reñé et al. (2017). The sequences obtained were deposited in GenBank under the Accession

183   Numbers: MT998435 (18S rDNA), MT998437 (ITS), and MT998436 (28S rDNA).

184

185   **Cross-infections.** The host range of the parasitoid strain E4 was examined by conducting cross-

186   infection experiments with 13 microplankton species from different algal groups (Table 1). The

187   experiments were conducted in 24 well plates, where three replicates were set for each host.

188   1.5 mL of host culture at stationary phase showing cellular abundance >10^3 cells mL^{-1} was

189   mixed with 0.4 mL of a dense mature chytrid culture with plenty of released zoospores and

190   nearly no original host (*K. foliaceum*) present**.** Incubation time for cross-infection experiments

191   was fixed at 10 days allowing at least 2 generations of the chytrid parasitoid. The susceptibility

192   of hosts to chytrid infection was defined by considering both, the capacity of the parasitoid to

193   kill the host, measured as the presence of new infections, and the capacity of the parasitoid to

194   exceed host growth rate, measured as the number of healthy host cells remaining in the well

195   after 10 days of parasitoid inoculation, being evaluated qualitatively. The wells were observed

196   after 2, 3, 5, 7 and 10 days of chytrid inoculation and susceptibility was classified qualitatively

197   into four categories following Lepelletier et al. 2014a: i) resistant, no infections were detected

198   within the host ii) low susceptibility, some infections were detected but more than 10 living

199   host cells remained in the well after 10 days, iii) moderate susceptibility, infections were

200   detected and less than 10 living host cells were observed in the well after 10 days and iv) high

201   susceptibility, no host cells persisted after 10 days.

202

203   **RESULTS**

204   The new chytrid dinoflagellate parasite described here was isolated from a typical dinoflagellate

205   dominated phytoplankton community containing 78.6% *K. foliaceum* of the total phytoplankton

206   biomass (Alacid et al. in press). A host-parasite system was successfully established by isolating

207   infected *K. foliaceum* cells and adding new cells from cultured isolates of this host species.

208   Strain E4 was a quite aggressive parasitoid in the co-culture, infecting the dinoflagellate host as

209   a typical chytridiomycete completing its life cycle within 3 days of incubation at 21 $^\text{o}$C.

210   **Phylogeny**

211   The 18S, 28S and 5.8S rDNA molecular information of the cultured chytrid was evaluated in

212   order to determine its phylogenetic position and relationships. All sequences showed low

213   similarity values with closest sequences, and thus, forming long branches in all phylogenies. In

214   fact, the 18S rDNA sequence showed a highest similarity of 89.5% with sequence AY601710

215   (*Rhizophydium brooksianum*), the 28S showed a highest similarity of 87.4% with sequences

216   JN049539 and JN049540 (Chytridiomycota sp.), and the 5.8S showed a highest similarity of 92%

217   with sequence DQ485639 (*Rhizophydium* sp. PL-AUS-12). A first phylogenetic exploration was

218   performed on a dataset containing concatenated 18S, 5.8S and 28S rDNA sequences of taxa

219   belonging to different Chytridiomycota groups (Fig. S1). The chytrid sequence clustered inside

220 the order Rhizophydiales, which was retrieved with high statistical support (maximum

221 likelihood bootstrap value = 94%/Bayesian posteriorly probability = 1). It showed a close

222 phylogenetic relationship with the sequence of *Rhizophydium* sp. MP8 (94%/1), belonging to

223 the family Globomycetaceae, and formed a cluster (94%/1) with sequences of species

224 belonging to diverse families, such as *Operculomyces laminatus*, *Rhizophydium booksianum*,

225 *Staurastromyces oculus* and *Uebelmesseromyces harderi*. Once its taxonomic affiliation was

226 obtained, a thorough determination of its phylogenetic relationships was performed using a

227 more extensive dataset of Rhizophydiales representatives. For the concatenated 5.8S – 28S

228 rDNA phylogeny (Fig. 1), it formed a sister branch, but showing moderate support (86%/1), with

229 Globomycetaceae representatives, clustering with maximum support and including *Globomyces*

230 *pollinis-pini*, *Rhizophydium* sp. MP8, and *Urceomyces sphaerocarpus* sequences. Phylogenetic

231 reconstructions were also performed for single genes. For 28S rDNA phylogeny (Fig. S2), it

232 clustered independently, but showing again a close relationship with Globomycetaceae

233 representatives with moderate/high support (69%/1). Sequences JN049539 and JN049540,

234 which had the highest similarity with our sequence, even though only showing 70% of query

235 cover, did not cluster close to the E4 sequence, but formed a sister branch with

236 Dinomycetaceae. Finally, the 18S rDNA phylogeny (Fig. S3) was constructed from a dataset

237 mainly comprising environmental sequences and some identified species in order to explore

238 the relationship of the new chytrid with environmental information. It did not show a close

239 relationship with Globomycetaceae or any known representatives, but with environmental

240 sequences, clustering with FN690503 sequence obtained from the Baltic Sea, even though

241 under low statistical support.

242 **General morphology**

243 Light microscopical observations of E4 strain infection by using bright field (BF), phase contrast

244 (Ph) and differential interference contrast (DIC) demonstrated that the vegetative life-cycle of

245 the parasitoid presented the following main stages: zoospores, cysts, young and mature

246 sporangia (Fig. 2). Zoospore body diameter is 3.9 – 4.8 μm (average 4.5) (n = 11), flagellar

247 length is 26 – 27 μm (n = 11) (Fig. 2A, B). Zoospores retract their flagella after attachment to the

248 host (Fig. 2C) and produce a cyst wall (Fig. 2D). In the cyst, a special structure can be seen,

249 measuring 1.2 μm (measured under LM), called here the syringe-like structure, or syringe,

250 which takes part in the attachment and, probably, immobilization of the prey (Fig. 2D).

251 The cyst germinates within the host forming a haustorium in the shape of an elongated balloon

252 with a thin layer of peripheral cytoplasm (Fig. 2E). The cyst forms a lateral bud, which enlarges

253 into a sporangium with a spiny surface (Fig. 2F). A cyst itself does not enlarge, probably because

254 of the thickening of its wall (see Fig. 5D). It becomes a papilla of the growing sporangium with a

255 thick and smooth wall in contrast to the main surface of sporangium which is covered by thorns

256 (Fig. 2F–I, K). The shape and surface of sporangia are better seen in SEM images (Fig. 3). The

257 place of parasite penetration into the host is located at the papilla base (Fig. 3C). The

258 sporangium enlarges (Fig. 2F–H) and matures producing 40 – 60 zoospores (Fig. 2I, J). We did

259 not observe zoospore release, but empty sporangia have a discharge pore with smooth ridges

260 (Fig. 2K; 3E). The distinctive lid which could cover this discharge pore was not found, but the

261 pore is covered with flat and thickened sporangial wall (see its ultrastructure below).

262 When a single parasite infects a host cell, the size of the mature spherical sporangium is about

263 $20 - 25 \ \mu m$ (n = 11), nearly as large as the host (Fig. 2G, H, J). However, when multiple

264 infections occurred in a single cell at different times, different stages of growing sporangia are

265 visible attached to the host surface (Fig. 3B, D).

266

267 **Zoospores**

268 Zoospores appear as a result of multinuclear sporangial division into uninuclear cells during

269 zoosporogenesis. Flagellar appearance in the cells does not mean that zoospores are mature

270 and ready to release. Immature zoospores have non-aggregated ribosomes (Fig. 4A). Mature

271 zoospores contain a central nucleus surrounded by a ribosomal core (Fig. 4B). In released

272 zoospores, the ribosomal core is surrounded and crossed by ER cisternae (Fig. 4C). One big

273 posterior lipid globule is partly submerged in the ribosomal core and closely associated with

274 lobed microbody forming a microbody-lipid complex (MLC) (Fig. 4C, E). Several mitochondrial

275 profiles locate around a ribosomal aggregate often in close association with it (Fig. 4D).

276 Numerous small vesicles with electron dense contents are spread throughout the cytoplasm.

277 The flagellar apparatus in the zoospores is closely associated with the MLC (Fig. 4E). Its

278 microtubular root passes from the flagellar base along the microbody surface (see Fig. 5 for

279 details). Released zoospores can be fed by amoebae: in some sections a zoospore was found in

280 the food cap of a contaminative amoeba (Fig. 4F). According to the distinctive ultrastructural

281 character, namely mitochondria with flat cristae surrounded by ER, this amoeba belongs to

282 Heterolobosea.

9

Flagellar apparatus

The structure of the flagellar apparatus, or kinetid, is an essential character for a new taxon description and phylogeny. The base of the flagellum at the posterior end of the cell is located very close to the microbody, which covers a lipid globule. A kinetid consists of the kinetosome with emergent flagellum and a non-flagellar centriole oriented parallel to the kinetosome (Fig. 5A–N). The proximal ends of both the kinetosome and centriole are merged in the saddle-like fibrillar sheath (Fig. 5D–F, J–N). The kinetosome and centriole are connected to each other by a prominent fibrillar bridge, which is rather thick and consists of several oblique fibrils without a crossing plate, or so called zone of convergence (Fig. 5C–E, L, M). The cartwheel organisation of nine microtubular triplets is present in the proximal end of both the kinetosome and centriole (Fig. 5E, F). The centriole is approximately two-thirds the kinetosome length (Fig. 5J, N). The distal end of kinetosome is connected to the plasma membrane by 9 unusually thick props, or transition fibers, which are interconnected to each other in their middle part (Fig. 5A, B, G–N). The flagellar transition zone is simple – it only comprises a thin transverse plate (Fig. 5J, K). The kinetosome produces at least one root of 6 microtubules associated with a short fibrillar plate at its base. The other side of the root (opposite to the fibrillar plate) is closely associated with the microbody surface (Fig. 5E–H, O–R).

Cyst and sporangium

Just after the flagellar retraction, the attached cell of E4 is covered by a loose and relatively thin wall and contains disordered microtubules of the flagellar axoneme (Fig. 6A). Disaggregated ribosomes, mitochondrial profiles with flat cristae, many small vesicles with electron dense contents and ER cisternae are visible in sections. The large lipid globule has an unusual structure. It is covered with thin electron dense material connected to the ER cisternae. A tube-like structure appears in the centre of the lipid globule at this stage of the cyst formation (Fig. 6 A). Following the cyst development, the lipid globule transforms into the syringe-like structure, and its central tube becomes the needle that will penetrate the host cell wall (Fig. 6B, C). The syringe consists of glass-like cylinder with electron dense walls and a concave bottom facing towards the plasma membrane; the cytoplasm inside the cylinder contains ER connected to the electron dense globules, which are associated with the needle. The syringe wall locates in a vacuole, and cytoplasm with ER, globules, and needle fill the glass. When the tube (needle) is extruding, it penetrates the cyst wall and the wall of the host (Fig. 6B, C). Details of the syringe structure are presented in the consecutive serial sections shown in Figure 7A–H. This structure

315 retained within the sporangium throughout sporangial development up to zoospore maturation

316 (Fig. 7I). Two syringes per cyst were rarely observed (Fig. 7K).

317 The papilla (former cyst) does not change its shape, its wall becomes much thicker and retains a

318 smooth surface (Fig. 6C, 7I), while the sporangium outgrows laterally having a wall covered with

319 spines of approx. 1.5 μm in length (Fig. 6D). A multinuclear sporangium contains numerous lipid

320 globules (Fig. 6F), which seem to disappear after multiple divisions on the uninuclear cells (Fig.

321 7I). The ribosomal core around the nucleus and the lipid globule appear in zoospores after

322 flagella formation (Fig. 4A, B; 6D, F, G; 7I).

323 In a mature sporangium a septum with pores appears in front of the funnel (Fig. 2H; 6F, G). It

324 separates the sporangium content from the haustorium.

325 Zoospore release takes place from a discharge pore, appearing in the mature sporangium as a

326 flat plot covered with thickened sporangial wall (Fig. 6F; 7I). We did not observe how it opens

327 and what occurs with this plot. The shape of the discharge pore is round with smooth ridges

328 and has rather a large diameter (approx. 10 μm) (Fig. 2K), which is enough for several zoospores

329 to come out at the same time. Therefore, a sporangium obviously does not break but somehow

330 opens to discharge a number of zoospores.

331 **Funnel**

332 The haustorium penetrates the host cell in close proximity to the syringe (Fig. 7I). It appears in

333 the cyst as an electron dense plate under the plasma membrane adjacent to the syringe (Fig.

334 7A, B). The ridges of the plate are connected to ER, and the initial plate is located in the flat

335 matrix vesicle (Fig. 7B, K). Then, the plate transforms into the funnel, which breaks the cyst wall

336 and the host wall and fixes the ridges of the hole in the host cell (Fig. 7J). The haustorium grows

337 through the funnel into the host transporting there the cytoplasm with mitochondria, ER

338 cisternae and lipid globules (Fig. 6E). Probably, the cytoplasm moves into the haustorium under

339 the pressure probably caused by the growing vacuole of the cyst (Fig. 6C, E). The haustorium

340 itself is actually a part of sporangium containing a big vacuole and peripheral cytoplasm with all

341 the cellular organelles and inclusions except the nucleus (Fig. 2F–H, J; 6E; 7I, J). It grows along

342 with the sporangium and finally replaces the host contents becoming nearly as large as the

343 mature sporangium.

344

345 **Cross-infections**

346 The strain E4 was detected infecting *Kryptoperidinium foliaceum* in field samples. However,

347 laboratory experiments were conducted to determine its potential to infect other

348 dinoflagellates, as well as other algae (Table 1). From all the species tested, only two

349 dinoflagellates were infected by E4, and they showed different susceptibility, which was

350 determined qualitatively**.** Among the seven dinoflagellate species tested, *K. foliaceum* showed a

351 high susceptibility to infections, with no living hosts after 10 days of parasite inoculation.

352 *Heterocapsa triquetra* was infected by E4 showing low susceptibility, i.e. only a few host cells

353 were infected. Infections were not observed for the other tested species belonging to

354 haptophytes, cryptophytes, chlorophytes and cyanobacteria, being resistant to chytrid

355 infections.

356 **DISCUSSION**

357 Parasitic chytrids are extensively recorded in aquatic ecosystems, both in marine and

358 freshwater environments (Amend et al. 2019). In freshwater, chytrids infect multiple

359 phytoplankton groups, like diatoms, green algae, and cyanobacteria (Kagami et al. 2007). A few

360 cases of Chytridiomycota infecting dinoflagellates are known. The freshwater dinoflagellate

361 *Peridinium gatunense* is infected by *Phlyctochytrium* sp. (Alster and Zohary 2007) and

362 *Dinochytrium kinnereticum* (Leshem et al. 2016). *Amphicypellus elegans* and *Rhizophydium*

363 *nobile* infect freshwater *Ceratium* species (Canter 1968, Canter and Heaney 1984).

364 *Rhizophydium echinatum* infects *Glenodinium cinctum* (Dangeard 1888). Here, we presented a

365 novel chytridiomycete isolated from brackish waters as a parasite of the dinophyte.

366 **Molecular phylogeny**

367 According to molecular phylogeny, based on 18S, 5.8S, and 28S rDNA sequences, strain E4

368 clusters inside Rhizophydiales in the Chytridiomycota dataset. In both 28S and 28S + 5.8S

369 Rhizophydiales datasets, it clusters close to saprotrophic *Globomyces* and *Urceomyces* with

370 moderate-high support (70%/1 and 82%/1, respectively), even though it forms a long branch in

371 comparison to others (Figs S1, S2). The phylogenetic position was consistent with all analyses

372 performed and did not show a strong relationship with any other representatives of known

373 families. The 18S tree including environmental sequences shows several uncultured lineages

374 around the E4, and forming a monophyletic cluster with other families like Globomycetaceae,

375 Operculomycetaceae, Staurastromycetaceae or Rhizophydiaceae (Fig. S3), a cluster also

376 observed for the other phylogenetic analyses performed in this study and recorded in the

377 literature (Van den Wyngaert et al. 2017, Garvetto et al. 2019). These results together with its

378   unique morphological characteristics support a new family within Rhizophydiales. Additionally,

379   the phylogenetic position did not show a close relationship with Dinomycetaceae, which

380   includes the only known species that infects dinoflagellates in brackish environments. Our

381   results show dinoflagellates can be affected by many different groups of Chytridiomycota, and

382   regarding Rhizophydiales, the two species known to infect dinoflagellates are not closely

383   related. It suggests that infections of dinoflagellates are not restricted to a specific phylogenetic

384   group and thus, the diversity of brackish chytrids infecting dinoflagellates is still largely

385   unknown and requires detailed studies to understand those interactions.

386   **Morphology and life cycle**

387   Strain E4 possesses typical features for chytridiomycete development within the host, which

388   can be described as a parasitoid of brackish dinoflagellates with a simple thallus, a monocentric

389   epibiotic sporangium having endogenous development, and with haustorium (Fig. 8). However,

390   its internal structure has several peculiar traits, which are discussed below.

391   **Syringe and funnel.** These unusual structures seem to be described for zoosporic fungi for the

392   first time. The function of the syringe could be the immobilization of the host cell after

393   zoospore attachment and encystment. The electron dense granule connected to the needle

394   inside the cylinder looks like a container for proteins transported in the granules from the ER.

395   These proteins being injected via the needle, could, probably, paralyze the prey, which stops

396   swimming and settles down upon infection. We found a maximum of two syringes per cell in

397   sections, but it was rarely observed, and normally one syringe per sporangium is present.

398   Further study of the syringe structure and function are needed to confirm the role it plays in

399   the infection process.

400   Among the chytridiomycetes, the rhizoid (or haustorium) penetration into the host is not

401   normally accompanied by special structures like the funnel (Powell 2016). Interestingly, the

402   haustorium itself can produce one more funnel at the distal end (Fig. 6E), the function of which

403   is unknown. A haustorium is quite rare among Rhizophydiales (Letcher and Powell 2012). It has

404   been described in *Rhizophydium skujai* (Skuja) Karling as being "…irregularly lobate,

405   transversely elongate, sac-like." According to the drawings reproduced by Letcher and Powell

406   (2012), *R. skujai* also had a large vacuole with peripheral cytoplasm around. *Chytridium*

407   *aggregatum* Karling (Karling 1938) and *Ch. sexuale* Koch (Koch 1951) also have a haustorium

408   named an apophysis. It is spherical and comparatively small in *Ch. sexuale*, but rather big and

409   elongated with rhizoids at the distal end in *Ch. aggregatum*.

410 **Papilla**. Papillae in chytrids normally serve for zoospore release, but in the case of E4 it is a

411 thick-walled chamber of the sporangium, developed from the cyst. Such a phenomenon was

412 described for a few chytridiomycetes *Ch. oedogonii* Couch and *Ch. aggregatum* Karling (Couch

413 1938, Karling 1938). While in *Ch. oedogonii* the rhizoid penetrates the host from the apical part

414 of the papilla, in *Ch. aggregatum* it is formed at the base of the papilla, like in E4. The sporangia

415 of *Ch. aggregatum* and E4 have a fairly similar shape and the rhizoidal system which appears

416 from the outgrowing young sporangium rather than from the cyst. The sporangium of *Ch.*

417 *aggregatum* is a bit smaller (10–18 µm vs 20–25 µm in E4) and its papilla is brownish, while it is

418 colourless in E4.

419 The septa with pores separating sporangial contents from rhizoid is a character of monoblephs

420 rather than chytrids (Powell 2016). It appears during zoospore maturation in E4 and is also

421 present in *Ch. aggregatum* (Karling 1938).

422 Both, *Ch. aggregatum* and E4 have a discharge pore which locates apically or subapically in *Ch.*

423 *aggregatum* and is covered by operculum. In E4 it is subapical, but has no specific structure

424 characteristic for the lid as e.g. in *Chytridium confervae* (Taylor and Fuller 1981). A flat plot in

425 the sporangium E4 is, in fact, the thickened sporangial wall having plano-convex profile (Fig. 6F;

426 7I) like that described for *Rhizophydium planktonicum* (Beakes et al. 1993), and we never saw

427 an empty sporangium with open lid. In *Globomyces pollinis-pini* and *Urceomyces sphaerocarpus*

428 forming a sister clade to E4 no lid-like structure was observed during zoospore discharge

429 (Letcher et al. 2008). Probably, a flat plot of sporangial wall dissolves before zoospore release.

430 **Taxonomy**

431 Strain E4 differs from other Rhizophydiales on account of its sporangium and feeding system:

432 its spiny sporangium has a smooth papilla as a remnant of the cyst; it has a large haustorium

433 with central vacuole and peripheral cytoplasm, rhizoids are absent. The cyst and sporangium

434 contain two unique structures, which do not occur in Chytridiomycetes: a syringe and a funnel.

435 The general zoospore structure is similar to that of other representatives of the order

436 Rhizophydiales in respect of: a nuclear associated ribosomal core, a single big lipid globule, but

437 without the rumposome (fenestrated cisterna), a centriole parallel to kinetosome, and a

438 characteristic microtubular root passing to the MLC with simple or lobate microbody (Letcher et

439 al. 2008, Lepelletier at al. 2014b). These traits characterise the representatives of *Globomyces*

440 *pollinis-pini* and *Urceomyces sphaerocarpus* (Letcher et al. 2008), which belong to the family

441 Globomycetaceae and form a sister clade to E4 (Fig. 1). For instance, the general disposition of

442   organelles in zoospores of E4 is similar to that in *Globomyces pollinis-pini*: a ribosomal core in

443   which the nucleus is embedded, multiple mitochondria outside the ribosomal mass, a single

444   lipid globule with a lobed microbody, a microtubular root, and distinct vesicles with uniformly

445   electron-dense contents in the peripheral cytoplasm (Letcher et al. 2008). At the same time, a

446   ribosomal core crossed by ER, saddle-like structure, interconnected thick props, 6-microtubule

447   root associated with basal fibrillar plate, an absence of rumposome and zone of convergence in

448   the bridge between centriole and kinetosome distinguish E4 zoospores and their flagellar

449   apparatus from those of Globomycetaceae.

450   Interlaced props have been described for *Rhizidium phycophilum* (Chytridiales), which also has

451   a centriole parallel to kinetosome, the same structure of the props, but the transverse plate is

452   very thick and the microtubular root was not shown for this species (Picard et al. 2009). The

453   sporangium also differs from that of E4: the surface has reticulate ornamentation, and there is

454   an absence of a papilla (Picard et al. 2009). A spiny sporangium has been described for

455   *Rhizophydium echinocystoides*, but its spines are much longer (15–25 μm vs. maximum 1.5 μm

456   in E4). The sporangium of *Rh. echinocystoides* also has a papilla, but it displays an apical

457   position and serves for zoospore release (Letcher and Powell 2012). Among Rhizophydiales,

458   only *Rhizophydium skujai* has an unbranched sac-like haustorium inside the freshwater host

459   alga *Aphanizomenon flos-aquae* (Letcher and Powell 2012). It has tiny zoospores (1.5–2 μm)

460   and a sporangium with smooth wall. The sporangium of saprotrophic *Rhizophydium punctatum*

461   has a lateral papilla and is similar to E4 size, but its wall is smooth, and the sporangium

462   produces a branched rhizoid (Golubeva 1988).

463   A sporangium formed as a lateral outgrowth from the encysted zoospore is rare (Couch 1938,

464   Karling 1938). As far as we know, the ultrastructure and molecular phylogeny of *Chytridium*

465   *aggregatum* Karling 1938, having a sporangium most similar to E4, has not yet been

466   studied.

467   Thus, morphological characters of E4 are quite peculiar: some of them, e.g. a syringe and

468   funnel, are unique for the class Chytridiomycetes, or even for all zoosporic fungi; other features

469   occur in different families of Rhizophydiales. Such an organism definitely represents a new

470   genus and species and belongs to a separated family within Rhizophydiales.

471

472   **Diagnosis**

473 **Ericiomycetaceae fam. nov. Karpov et Reñé** (Rhizophydiales) MycoBank MB 836465.

474 Parasitic brackish-water chytrid. Sporangium formed as a lateral outgrowth from the encysted

475 zoospore. Zoospore has kinetosome with anterior microtubular root associated with short basal

476 fibrillar plate, ribosomal core ramified and crossed by endoplasmic reticulum.

477

478 *Ericiomyces* **gen. nov. Karpov et Reñé**

479 MycoBank MB 836466.

480 Parasitoid of brackish-water dinoflagellates with simple thallus with monocentric, epibiotic

481 sporangium having endogenous development, with haustorium. Sporangium covered with

482 spines has a smooth papilla. Zoospore with central ribosomal aggregation around the nucleus.

483 Posterior Microbody-Lipid-Complex (MLC) contains a lobed microbody enveloping a large lipid

484 globule. Mitochondria locate around ribosomal core. Kinetid is adjacent to the MLC. Centriole is

485 connected to kinetosome by oblique fibrils without zone of convergence. Anterior root

486 composed of six microtubules passes from kinetosome along the microbody. Cyst contains a

487 syringe-like structure, and uses a special funnel-shaped structure for penetration into the host.

488 Etymology. *Ericio* (Greek) – meaning hedgehog, refers to the spiny sporangium appearance,

489 *myces* – fungus.

490 Type species *Ericiomyces syringoforeus* sp. nov.

491 *Ericiomyces syringoforeus* **sp. nov. Karpov et Reñé**

492 MycoBank MB 836467. GenBank numbers: MT998435 (18S rDNA), MT998437 (ITS), MT998436

493 (28S rDNA). Figures 2–7.

494 Parasitoid of dinophytes, with some preference for *Kryptoperidinium* species. Mature epibiotic

495 spherical spiny sporangium of 20 – 25 μm in diameter with smooth lateral papilla. Spines are up

496 to 1.5 μm in length. Spherical zoospores of 3.9 – 4.8 μm in diameter with a posterior lipid

497 globule, flagellum is 26 – 27 μm. Zoospores are released through a discharge pore appr. 10 μm

498 in diameter. Syringe-like structure is 1.2 μm long.

499 Etymology. From the Greek σύριγγα *syringa* – syringe, and φορέας *foreus* – carrier, the unique

500 organelle for infection.

501 Type strain: E4, isolated on the host *Kryptoperidinium foliaceum* from samples collected in

502 Kökar, located in Åland Archipelago (SW coast of Finland) in the northern Baltic Sea in June

503 2016.

504 Holotype: a fixed specimen derived from the strain E4 embedded in a resin block for electron

505 microscopy deposited in the CCPP ZIN RAS under the No X-135.

506 **Ecology**

507 *Ericiomyces syringoforeus* appeared in samples obtained during a bloom of the dinoflagellate

508 *Kryptoperidinium foliaceum*. Concurrently, other parasites were present in those samples

509 infecting the same host, e.g. *Parvilucifera catillosa*, an endoparasitoid belonging to the

510 Perkinsozoa (Alveolata) (Alacid et al. in press). Thus, fungal parasitism is not the only factor

511 involved in the changes of population dynamics of the dinoflagellate, which can be attacked

512 and affected by different co-occurring parasites. In both cases, infections were observed after

513 the incubation of the natural samples in the laboratory and to the best of our knowledge, it

514 represents the first record of co-occurring chytrid-perkinsid species simultaneously infecting

515 the same host. Unfortunately, the prevalence of each species in the natural population could

516 not be determined but cross-infection experiments showed the chytrid was able to infect

517 efficiently *K. foliaceum*, as well as *H. triquetra*, while infections were not observed on other

518 phytoplankton species tested. Those same host species were tested for infections of *P. catillosa*

519 (Alacid et al. in press), showing exactly the same results on susceptibility. Thus, it confirms that

520 both parasites are competing for the same resources. Cross-infection experiments were also

521 performed for *D. arenysensis* (Lepelletier et al. 2014b). Only positive results were obtained for

522 dinoflagellate representatives, being able to infect 31 different strains out of 48 tested,

523 belonging to 13 different species. However, *K. foliaceum* was not infected by *D. arenysensis*.

524 Even though there is a bias in the number of species tested in the cross-infection experiment,

525 both species showed remarkable differences regarding their host preferences. Further studies

526 should focus in the role of parasitism in dinoflagellate population dynamics and understanding

527 those fluxes would help to elucidate the mechanisms of blooms development.

528

551 **References**

552 Alacid E, Reñé A, Gallisai R, Paloheimo A, Garcés E, Kremp A (in press) Description of two new

553 coexisting parasitoids of blooming dinoflagellates in the Baltic sea: *Parvilucifera catillosa* sp.

554 nov. and *Parvilucifera* sp. (Perkinsea, Alveolata). Harmful Algae

555 Alster A, Zohary T (2007) Interactions between the bloom-forming dinoflagellate *Peridinium*

556 *gatunense* and the chytrid fungus *Phlyctochytrium* sp. Hidrobiologia 578:131–139

557 Amend A, Burgaud G, Cunliffe M, Edgcomb VP, Ettinger CL, Gutiérrez MH, Heitman J, Hom

558 EFY, Ianiri G, Jones AC, Kagami M, Picard KT, Quandt CA, Raghukumar S, Riquelme M, Stajich J,

559 Vargas-Muñiz J, Walker AK, Yarden O, Gladfelter AS (2019) Fungi in the marine environment:

560 open questions and unsolved problems. mBio 10:e01189–18.

561 https://doi.org/10.1128/mBio.01189-18.

562 Beakes GW, Canter HM, Jaworski GHM (1993) Sporangium differentiation and zoospore fine-

563 structure of the chytrid *Rhizophydium planktonicum*, a fungal parasite of *Asterionella formosa.*

564 Mycol Res 97:1059–1074.

565 Canter HM (1968) Studies on British chytrids. XXVIII. *Rhizophydinium nobile* sp. nov.,

566 parasitic on the resting spore of *Ceratium hirundinella* O.F.Müll. from the plankton. Proc Linn

567 Soc Lond 179:197–201.

568 Canter HN, Heaney SI (1984) Observations on zoosporic fungi of *Ceratium* spp. in lakes of the

569 English Lake District; importance for phytoplankton population dynamics. New Phytol 97:601–

570 612.

571 Capella-Gutiérrez S, Silla-Martínez JM, Gabaldón T (2009) trimAl: a tool for automated

572 alignment trimming in large-scale phylogenetic analyses. Bioinformatics 25:1972–1973

573 Comeau AM (2016) Novel chytrid lineages dominate fungal sequences in diverse marine and

574 freshwater habitats. Sci Rep 6:30120.

575 Couch JN (1938) A new species of Chytridium from Mountain Lake, Virginia. Jour

576 Elisha Mitchell Sci Soc 64:256–259.

577 Kremp A, Lindholm T, Dressler N, Erler K, Gerdts G, Eirtovaara S, Leskinen E (2009). Bloom

578 forming *Alexandrium ostenfeldii* (Dinophyceae) in shallow waters of the Åland Archipelago,

579 Northern Baltic Sea. Harmful Algae 8:318–328.

580 Dangeard P-A (1888) Recherches sur les algues inférieures. Annales des Sciences Naturelles

581 Botanique 7:105–175.

582 Frenken T, Alacid E, Berger S, Bourne EC, Gerphagnon M, Grossart H-P, Gsell AS, Ibelings

583 BW, Kagami M, Kupper FC, Letcher PM, Loyau A, Miki T, Nejstgaard JC, Rasconi S, Reñé A,

584 Rohrlack T, Rojas-Jimenez K, Schmeller D, Scholz B, Seto K, Sime-Ngando T, Sukenik A, Van de

585 Waal DB, Van den Wyngaert S, Van Donk E, Wolinska J, Wurzbacher C, Agha R (2017)

586 Integrating chytrid fungal parasites into plankton ecology. Research gaps and needs.

587 Environmental Microbiology 19:3802–3822.

588 Garvetto A, Badis Y, Perrineau MM, Rad-Menéndez C, Bresnan E, Gachon CM (2019) Chytrid

589 infecting the bloom-forming marine diatom *Skeletonema* sp.: Morphology, phylogeny and

590 distribution of a novel species within the Rhizophydiales. Fungal biology 123:471–480.

591 Gleason FH, Jephcott TG, Küpper FC, Gerphagnon M, Sime-Ngando T, Karpov S, Guillou L,

592 Van Ogtrop FF (2015) Potential roles for recently discovered chytrid parasites in the dynamics

593 of harmful algal blooms. Fungal Biology Reviews 29:20–33.

594 Golubeva OG (1995) Keys to mushrooms of Russia. Class Chytridiomycetes. Issue 1. SPb,

595 "World and Family-95" (in Russian)

596   Hakanen P, Suikkanen S, Franzén J, Franzén H, Kankaanpää H, Kremp A (2012) Bloom and

597 toxin dynamics of Alexandrium ostenfeldii in a shallow embayment at the SW coast of Finland,

598 northern Baltic Sea. Harmful Algae 15:91–99.

599   Hansen G, Daugbjerg N, Henriksen P (2000) Comparative study of *Gymnodinium mikimotoi*

600 and *Gymnodinium aureolum*, comb. Nov. (=*Gyrodinium aureolum*) based on morphology,

601 pigment composition, and molecular data. J Phyc 36:394–410.

602   Jones EBG, Suetrong S, Sakayaroj J, Bahkali A, Abdel-Wahab M, Boekhout T, Pang K-L (2015)

603 Classification of marine Ascomycota, Basidiomycota, Blastocladiomycota and Chytridiomycota.

604 Fungal Divers 73:1–72.

605   Jones EBG, Pang K, Abdel-Wahab MA *et al.* (2019) An online resource for marine

606 fungi. Fungal Divers 96**:**347–433. https://doi.org/10.1007/s13225-019-00426-5

607   Kagami M, de Bruin A, Ibelings BW, Van Donk E (2007) Parasitic chytrids: their effects on

608 phytoplankton communities and food-web dynamics. Hydrobiologia 578:113– 129.

609   Karling JS (1938) Two new operculate chytrids. Mycologia 30:302–312.

610   Karpov SA, Lopez-Garcıa P, Mamkaeva MA, Tcvetkova VS, Vishnyakov AE, Klimov VI, Moreira

611 D (2018) The chytrid-like parasites of algae *Amoeboradix gromovi* gen. et sp. nov. and

612 *Sanchytrium tribonematis* belong to a new fungal lineage. Protist 169:122–140.

613   Katoh K, Rozewicki J, Yamada KD (2019) MAFFT online service: multiple sequence alignment,

614 interactive sequence choice and visualization. Briefings in Bioinformatics 20:1160–1166.

615   Koch WJ (1951) Studies of the Chytridium, with observations on the sexually reproducing

616 species. Journal of the Elisha Mitchell Scientific Society 67:267–278.

617   Lazarus KL, James TY (2015) Surveying the biodiversity of the Cryptomycota using a targeted

618 PCR approach. Fungal Ecology 14:62–70.

619   Le Calvez T, Burgaud G, Mahé S, Barbier G, Vandenkoornhuyse P (2009) Fungal diversity in

620 deep-sea hydrothermal ecosystems. Appl Environ Microbiol 75:6415– 6421.

621 https://doi.org/10.1128/AEM.00653-09.

622   Lepelletier F, Karpov SA, Alacid E, Le Panse S, Bigeard E, Garcés E, Jeanthon C, Guillou L

623 (2014b) *Dinomyces arenysensis* gen. et sp. nov. (Rhizophydiales, Dinomyceataceae fam. nov.), a

624 chytrid infecting marine dinoflagellates. Protist 165: 230–244.

625   Lepelletier F, Karpov SA, Le Panse S, Bigeard E, Skovgaard A, Jeanthon C, Guillou L (2014a)

626   *Parvilucifera rostrata* sp. nov. (Perkinsozoa), a novel parasitoid that infects planktonic

627   dinoflagellates. Protist 165:31–49.

628   Leshem T, Letcher PM, Powell MJ, Sukenik A (2016) Characterization of a new chytrid species

629   parasitic on the dinoflagellate, *Peridinium gatunense*. Mycologia 108:731–743.

630   Letcher PM, Powell MJ (2012) A taxonomic summary and revision of Rhizophydium

631   (Rhizophydiales, Chytridiomycota). Alabama University Printing, No. 1. Imprint Tuscaloosa, AL.

632   Letcher PM, Powell MJ, Davis WJ (2015) A new family and four new genera in Rhizophydiales

633   (Chytridiomycota). Mycologia 107:808–830

634   Letcher PM, Velez CG, Barrantes ME, Powell MJ, Churchill PA, Wakefield WS (2008)

635   Ultrastructural and molecular analyses of Rhizophydiales (Chytridiomycota) isolates from North

636   America and Argentina. Mycological Research 112:759–782.

637   Picard KT, Letcher PM, Powell MJ. (2009) *Rhizidium phycophilum*, a new species in

638   Chytridiales. Mycologia 101:696–706.

639   Picard KT (2017) Coastal marine habitats harbor novel early-diverging fungal diversity. Fungal

640   Ecology 25:1–13.

641   Powell MJ (1974) Fine structure of plasmodesmata in a chytrid. Mycologia 66:606–614.

642   Powell MJ (2016) Chytridiomycota. In: Archibald *et al*. (ed.), Handbook of the Protists.

643   Springer International Publishing, Cham, Switzerland, pp 1–36.

644   Powell MJ, Gillette L (1987) Septal structure of the chytrid *Rhizophlyctis harderi*. Mycologia

645   79:635–639.

646   Raghukumar S (2017) Fungi in Coastal and Oceanic Marine Ecosystems. Marine Fungi.

647   Springer International Publishing AG. DOI 10.1007/978-3-319-54304-8. ISBN 978-3-319-54303-1

648   ISBN 978-3-319-54304-8 (eBook) Diversity of various groups of marine fungi (Raghukumar,

649   2017):25.

650   Reñé A, Alacid E, Figueroa RI, Rodríguez F, Garcés E (2017) Life-cycle, ultrastructure, and

651   phylogeny of *Parvilucifera corolla* sp. nov. (Alveolata, Perkinsozoa), a parasitoid of

652   dinoflagellates. Europ J Prot 58:9–25.

653   Richards TA, Leonard G, Mahé F, del Campo J, Romac S, Jones MDM, Maguire F, Dunthorn

654   M, De Vargas C, Massana R, Chambouvet A (2015) Molecular diversity and distribution of

655   marine fungi across 130 European environmental samples. Proc Biol Sci 282:2015–2243.

656   https://doi.org/10.1098/rspb.2015.2243.

657   Richards TA, Jones MDM, Leonard G, Bass D (2012) Marine fungi: their ecology and

658 molecular diversity. Annu Rev Mar Sci 4:495–522. https://doi.org/10.1146/annurev-marine-

659 120710-100802.

660   Scholin CA, Herzog M, Sogin M, Anderson DM (1994) Identification of group- and strain-

661 specific genetic markers for globally distributed Alexandrium (Dinophyceae). II. Sequence

662 analysis of a fragment of the 28S rDNA. Journal of phycology 30:999–1011.

663   Scholz B, Guillou L, Marano AV, Neuhauser S, Sullivan BK, Karsten U, Küpper FC, Gleason FH

664 (2016) Zoosporic parasites infecting marine diatoms – A black box that needs to be opened.

665 Fungal Ecology 19:59–76.

666   Taylor JW, Fuller MS (1981) The Golgi apparatus, zoosporogenesis, and development of the

667 zoospore discharge apparatus of *Chytridium confervae*. Exp Mycol 5: 35–59.

668   Van den Wyngaert S, Seto K, Rojas-Jimenez K, Kagami M, Grossart H-S (2017) A new

669 parasitic chytrid, *Staurastromyces oculu*s (Rhizophydiales, Staurastromycetaceae fam. nov.),

670 infecting the freshwater desmis *Staurastrum* sp. Protist 168:392–407.

671   Vélez CG, Letcher PM, Schultz S, Powell MJ, Churchill PF (2011) Molecular phylogenetic and

672 zoospore ultrastructural analyses of *Chytridium olla* establish the limits of a monophyletic

673 Chytridiales Mycologia. Mycologia 103:118–130.

674   White TJ, Bruns T, Lee SJWT, Taylor J (1990) Amplification and direct sequencing of fungal

675 ribosomal RNA genes for phylogenetics. PCR protocols: a guide to methods and

676 applications 18:315–322.

677

678

679

680

681

682

683

684

685

686

687 **Table 1.** Cross-infections between the chytrid *Ericiomyces syringoforeus* and selected hosts

688 belonging to different phytoplankton lineages. The susceptibility of each species was

689 determined qualitatively following Lepelletier et al. 2014a. Resistant: -; low susceptibility: +;

690 moderate susceptibility: ++; high susceptibility: +++.

Algal group	Host species	Strain	Susceptibility
Dinoflagellate	*Alexandrium ostenfeldii*	AOF0908	---
	Heterocapsa triquetra	HTF1002	+
	Kryptoperidinium foliaceum	KFF1002	+++
	Levanderina fissa	GFF1101	---
	Prorocentrum sp.	KVDAN31	---
	Karlodinium veneficum	Proro 1	---
	Pfiesteria piscicida	PPF02	---
Haptophyte	*Pleurochrysis roscoffensis*	Cocco 3	---
Cryptophyte	*Rhodomonas* sp.	Crypto07B1	---
	Rhinomonas nottbeckii	Crypto07B6	---
Chlorophyte	*Chlorella pyrenoidosa*	TV216	---
	Monoraphidium sp.	TV70	---
Cyanobacteria	*Aphanizomenon* sp.	KAC28	---

691

692

693

694

695

696

697

698

699

700

701

702

703

704

705

706

707
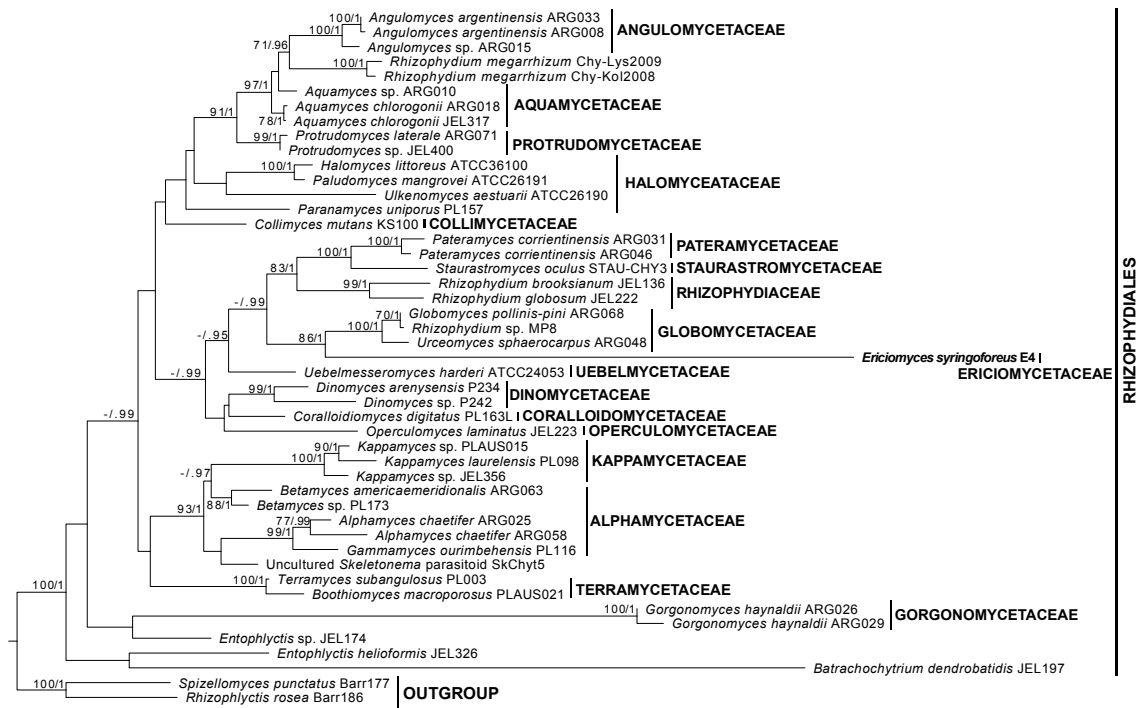
708

709 Fig. 1. Maximum likelihood phylogenetic tree of concatenated 5.8S, 18S and 28S rDNA

710 sequences representing the diversity of Rhizophydiales order. The sequence of *Ericiomyces*

711 *syringoforeus* is in bold. Statistical support of the nodes is presented by the bootstrap value (%)

712 and the Bayesian posterior probability. Only values >70% and >0.95 respectively are shown.

713 When only one of the values is below the threshold, it is indicated with a dashed line.

714

715

716

717

718

719

720

721

722

723

724

725

726

727

24
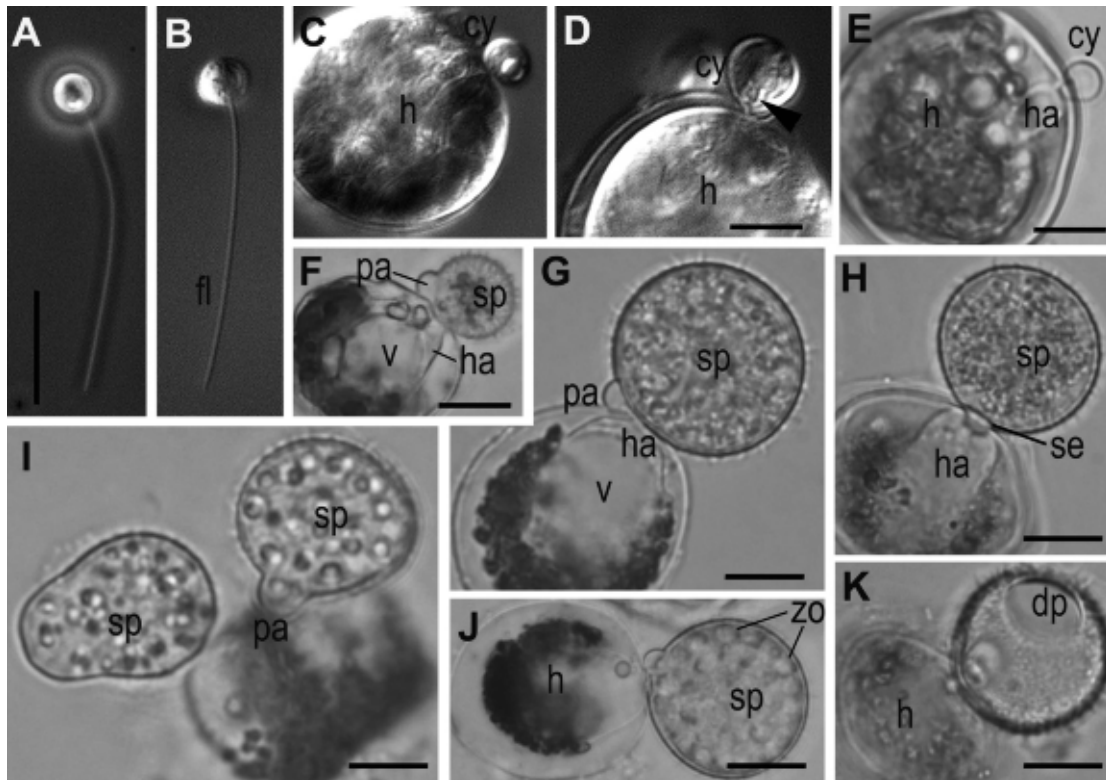
Fig. 2. Light microscopic images of the life-cycle stages of *Ericiomyces syringoforeus*. A,B – zoospores at Ph (A) and DIC (B); C – zoospore with retracted flagellum recently attached to the host (DIC); D – encysted zoospore with syringe (arrowhead) (DIC); E – encysted and germinated cell with haustorium (BF); F – young spiny sporangium with papilla; G,H – multinucleate immature sporangium with developed haustorium and septa (H); I,J – mature sporangia with formed zoospores (J); K – empty sporangium with a discharge pore after zoospore release. E–K – BF images.

Scales: A–C, E, G–K – 10 μm, D – 5 μm, F – 15 μm.

Abbreviations: am-amoeba, br-bridge, c-centriole, cy-cyst, dp-discharge pore, dv-dense vesicles, er-endoplasmic reticulum, fc-food cap, fl-flagellum, fu-funnel, h-host, ha-haustorium, k-kinetosome, l-lipid globule, m-mitochondrion, ma-microtubules of the axoneme, mi-microbody, mr-microtubular root, n-nucleus, ne-needle of the syringe, pa-papilla, pl-plate at the base of microtubular root, pr-props, rc-ribosomal core, s-spines, se-septa, sa-saddle, sp-sporangium, sr-subunits of ribosomes, sw-sporangial wall, sy-syringe, v-vacuole, zo-zoospore.
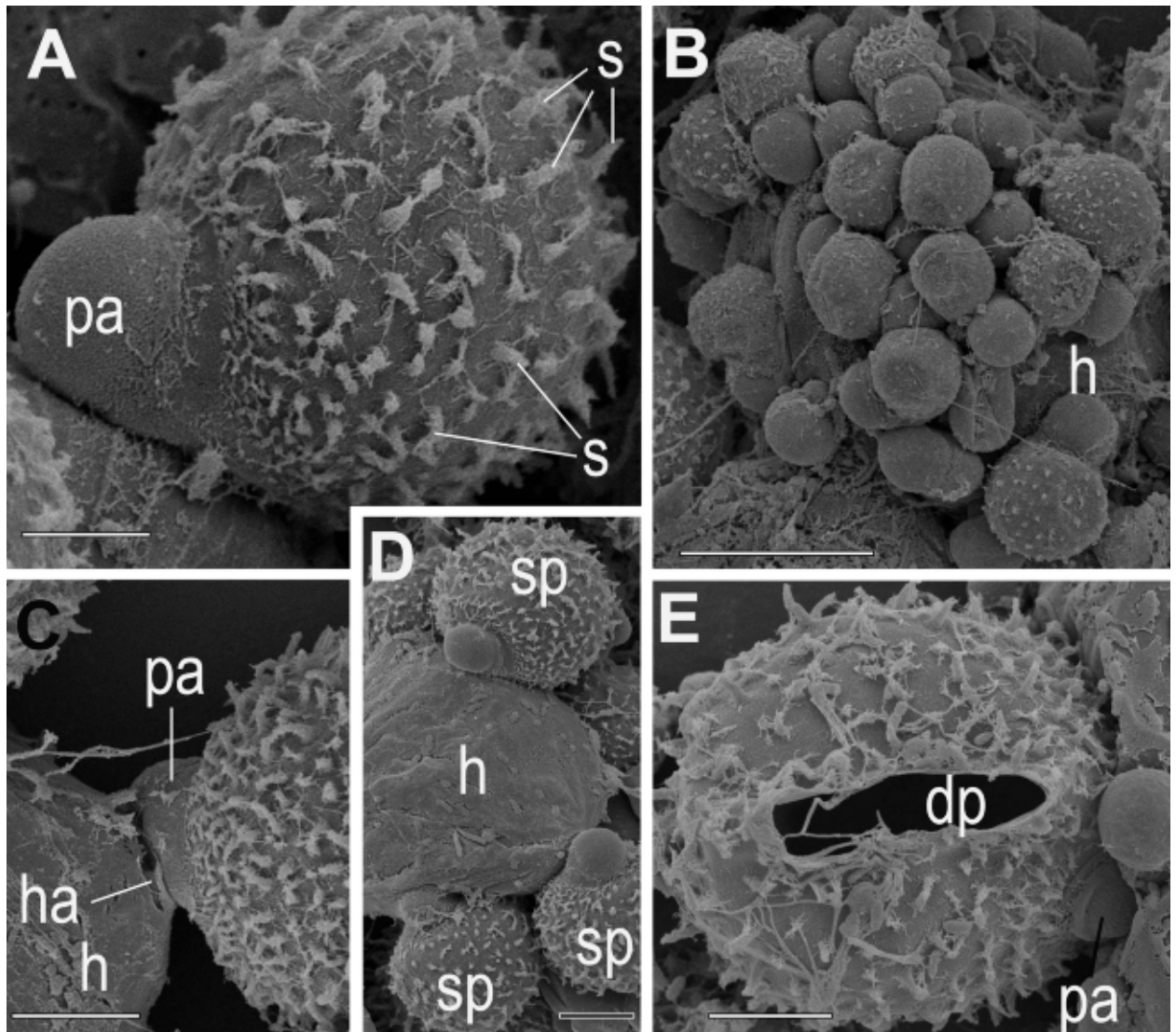
Fig. 3. Scanning electron microscopical images of sporangia and cysts of *Ericiomyces syringoforeus*. A – typical shape of spiny sporangium with papilla on the host surface; B – multiple infection of the *Kryptoperidinium foliaceum* cell (h), covered by cysts and early sporangia; C – haustorium penetration into the host; D – several growing spiny sporangia on host surface; E – empty sporangium with a discharge pore after zoospore releasing and papilla. Scales: A, C–E – 5 μm, B – 10 μm.
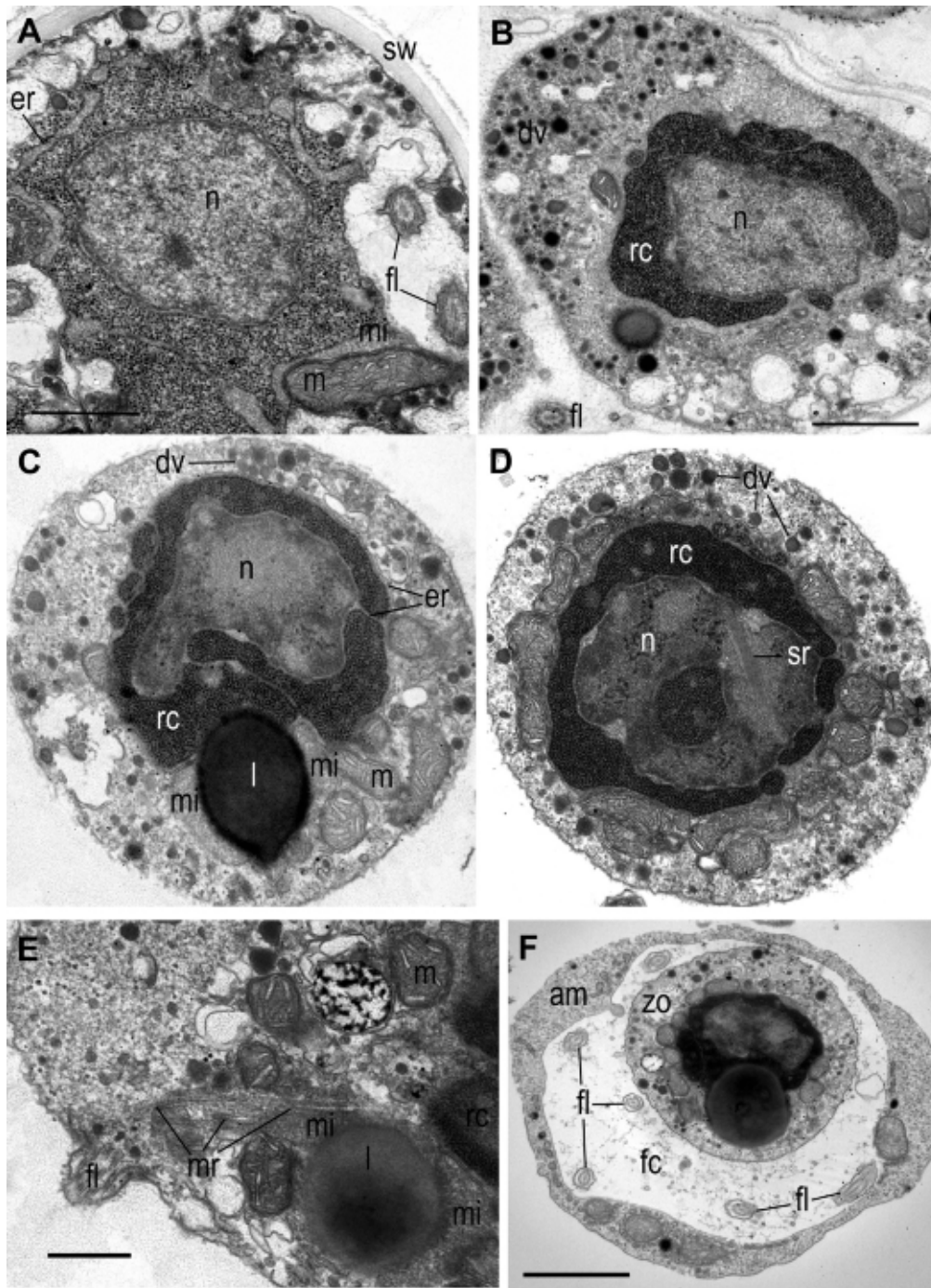
Fig. 4. General zoospore structure of *Ericiomyces syringoforeus* at ultrathin sections. A –
intrasporangial nearly mature zoospore but still with dispersed ribosomes; B - intrasporangial
mature zoospore with aggregated ribosomes; C, D – released zoospore structure; E – posterior
end of released zoospore with flagellum and anterior microtubular root; F – zoospore in the
food cup of heterolobosean amoeba.

Scales: A – 1 µm, B–D – 1 µm, E – 500 nm, F – 2 µm.
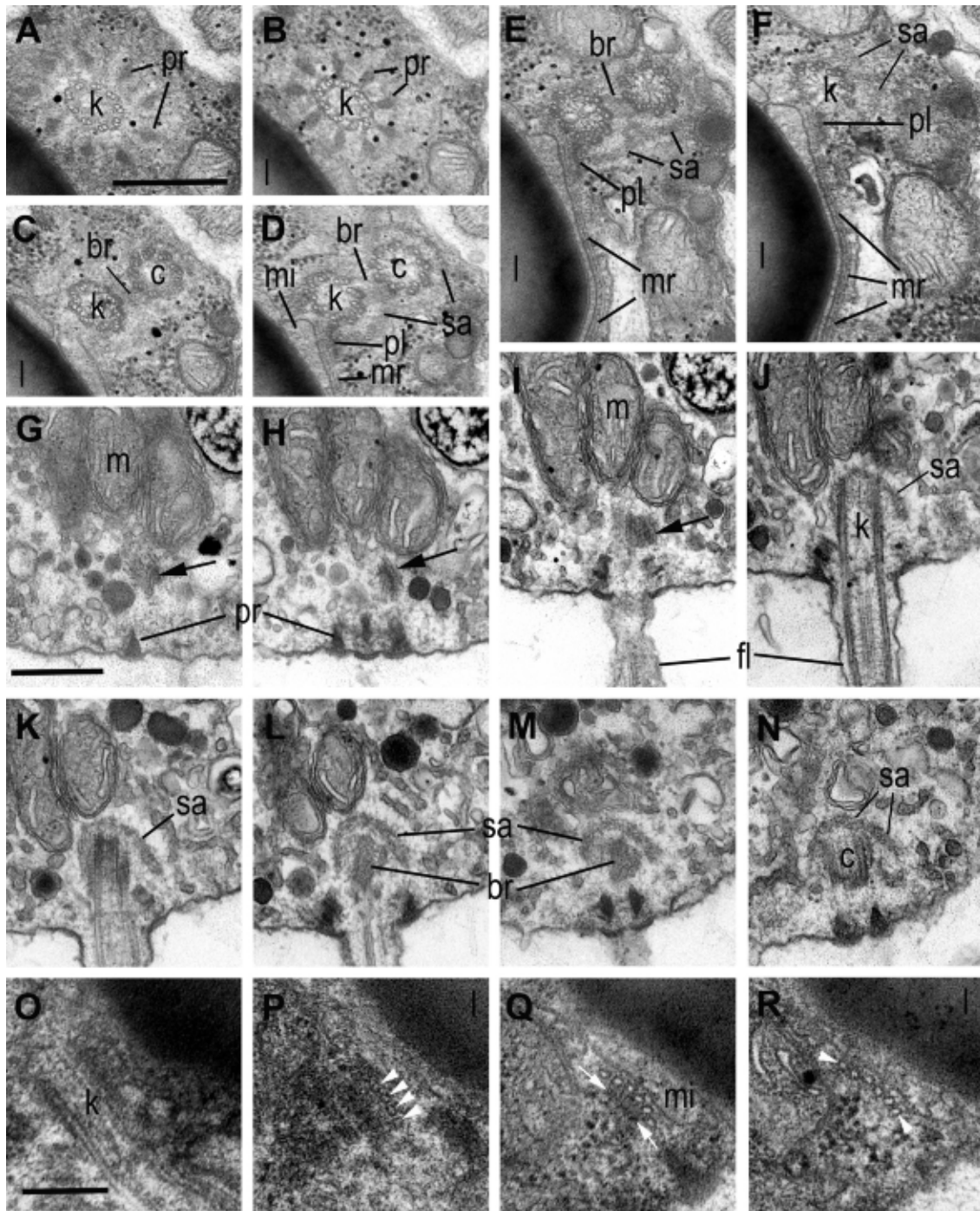
Fig. 5. Flagellar apparatus structure in zoospore of *Ericiomyces syringoforeus*. A–F – consecutive transversal sections of kinetosome and centriole in direction from distal to proximal end; G–N – consecutive longitudinal sections of kinetosome and centriole, arrows show oblique section of microtubular root with plate; O–R – consecutive transversal sections of microtubular root (bars) and its basal plate (arrowheads) in direction from its origin at kinetosome to distal end. Scales: A–F – 400 nm, G–N – 400 nm, O–R – 150 nm.
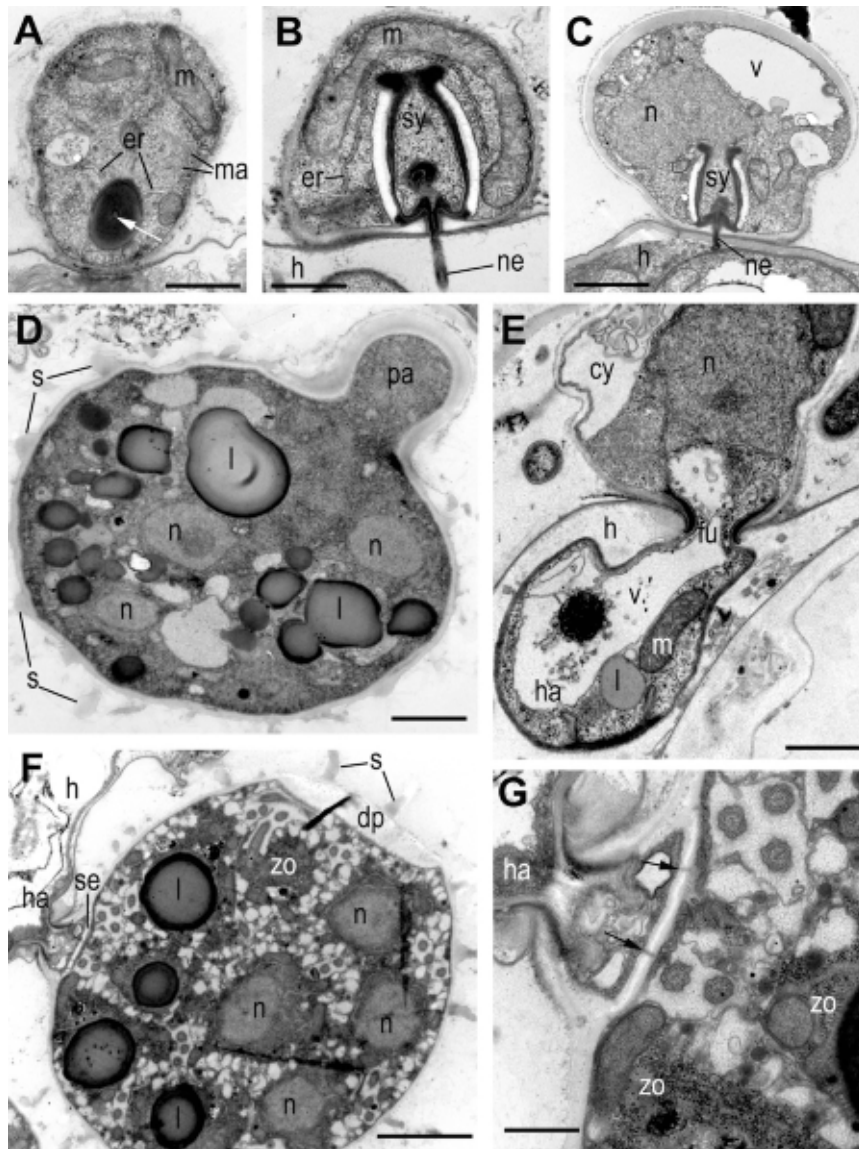
779

780 Fig. 6. Cyst and sporangia structure of *Ericiomyces syringoforeus* at ultrathin sections. A –

781 recently encysted zoospore with lipid globule containing a tube in the centre (white

782 arrowhead); B – cyst with mature syringe penetrating the host wall. C – part of sporangium

783 near the papilla with thickened wall and mature syringe penetrating the host wall; D –

784 immature multinucleate sporangium with papilla; E – sporangium with rhizoid fixed in the host

785 cell wall by funnel structure; F – mature sporangium with zoospores septa, funnel and

786 discharge pore; G – structure of septa at higher magnification. Arrows show the pores in septa.

787 Scales: A – 800 nm, B – 500 nm, C – 1 μm, D – 2.5 μm, E – 800 μm, F – 2 μm, G – 500 nm.

788

789

790

791
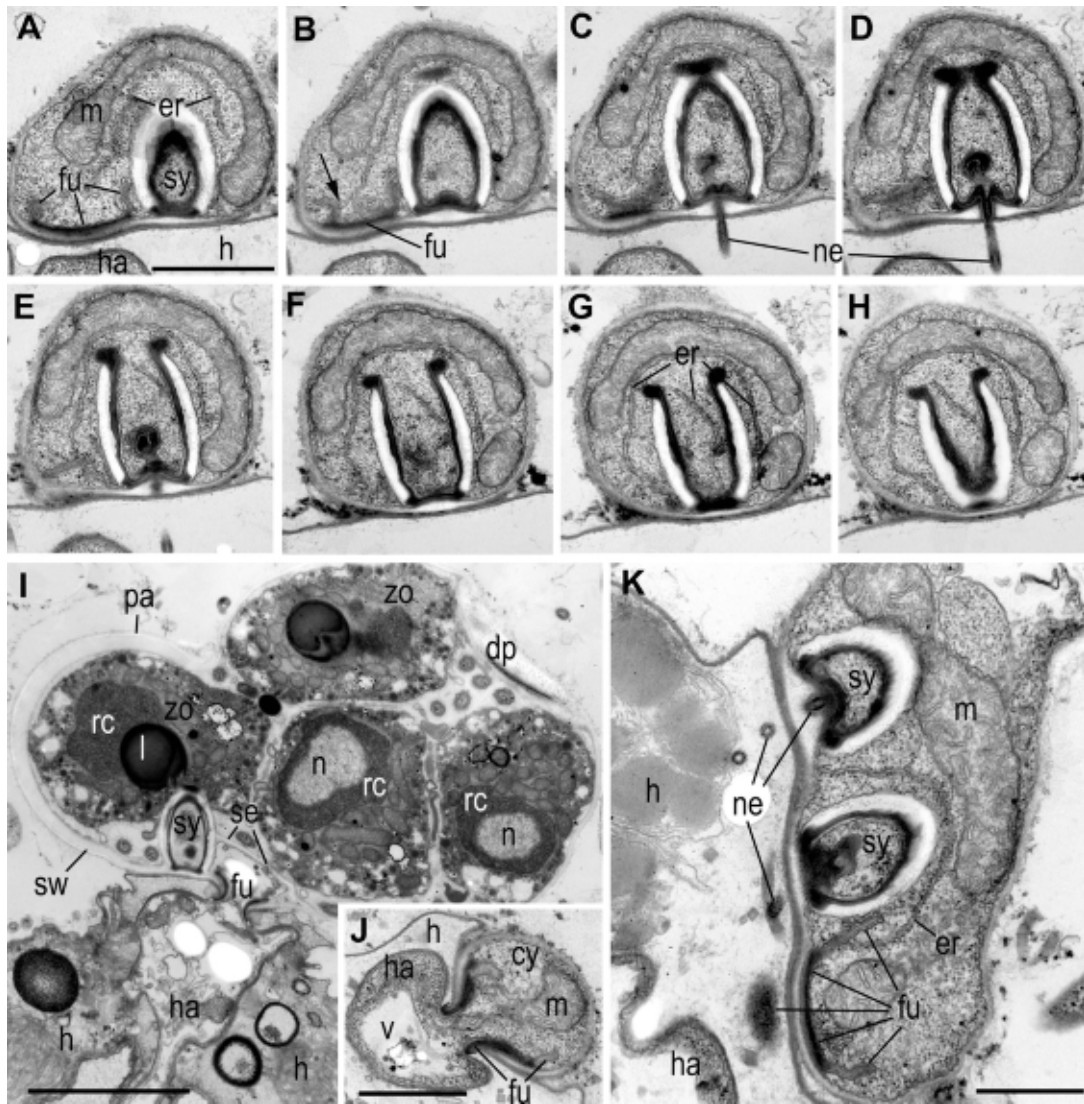
Fig. 7. Structure of syringe of *Ericiomyces syringoforeus* at the ultrathin sections. A–H – serial longitudinal sections of syringe in the cyst. Arrow on B shows ER connection with funnel. I – sporangium with mature zoospores contains an old syringe and funnel with haustorium. J – funnel-shaped structure in the cyst. K – part of young sporangium with two syringes and penetrative funnel.

Scales: A–H – 1 μm, I – 2 μm, J, K – 400 nm.
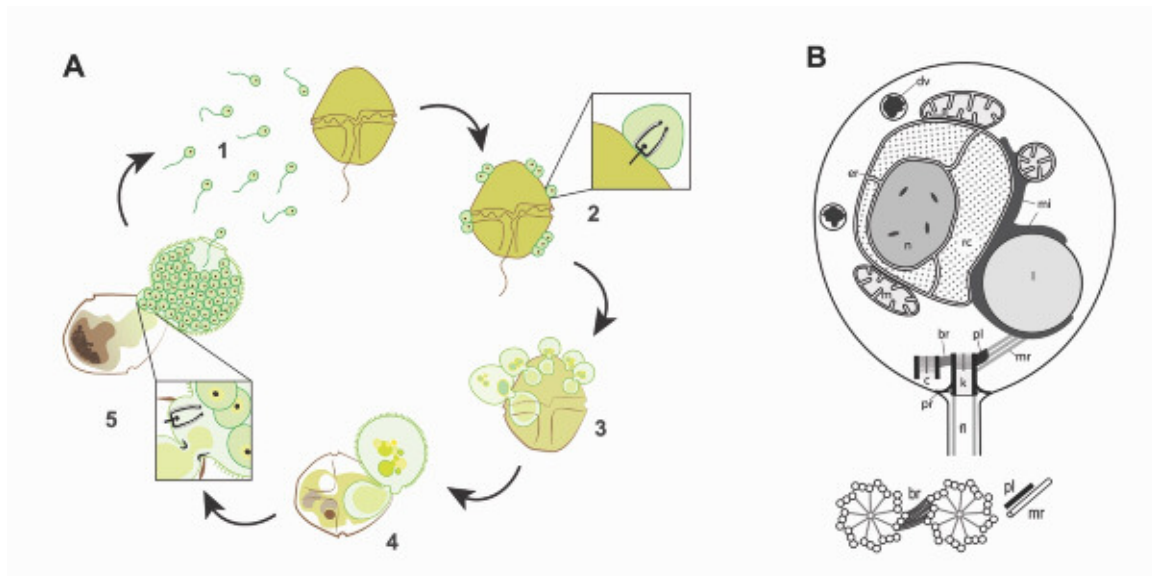
806
807
808 Fig. 8. Scheme of *Ericiomyces syringoforeus* life cycle (A) and zoospore structure (B).
809 1 – zoospores released from sporangium and move to another host, 2 – encysted zoospores on
810 the host surface (enlarged: syringe in the cyst paralyzing the host), 3 – five young sporangia
811 with haustoria feeding on the host, 4 – developed sporangium, 5 – mature sporangium
812 releasing zoospores (enlarged: sporangium/host interface).
813 Greenish color marks parasitoid, yellowish – healthy dinophyte, brownish – infected and
814 degraded dinophyte with brown theca.
815
816
817
818
819
820
821
822
823
824
825
826
827
828

832 Supplementary Figure 1: Maximum likelihood phylogenetic tree of concatenated 18S + 5.8S +

833 28S rDNA sequences representing the diversity of Chytridiomycota. The sequence of

834 *Ericiomyces syringoforeus* is in bold. Statistical support of the nodes is presented by the

835 bootstrap value (%) and the Bayesian posterior probability. Only values >70% and >0.95

836 respectively are shown. When only one of the values is below the threshold, it is indicated with

837 a dashed line.

838

839

840

841

842

843

844

845

846

847

848

849

850

851

852   Supplementary Figure 2: Maximum likelihood phylogenetic tree of 28S rDNA sequences

853   representing the diversity of the Rhizophydiales. The sequence of *Ericiomyces syringoforeus* is

854   in bold. Statistical support of the nodes is presented by the bootstrap value (%) and the

855   Bayesian posterior probability. Only values >70% and >0.95 respectively are shown. When only

856   one of the values is below the threshold, it is indicated with a dashed line.

857

858

859

860

861

862

863

864

865

866

867

868

RHIZOPHYDIALES

GQ995436 Uncultured Chytridiomycota clone T6P2AeE03
GQ995434 Uncultured Chytridiomycota clone T6P2AeF10
GQ995435 Uncultured Chytridiomycota clone T5P2AeB10
GQ995433 Uncultured Chytridiomycota clone T3P1AeB07
GQ995445 Rhizophydiales sp. AF033
JN940937 *Kappamyces* sp. BR 316
Betamyces sp. Barr-316
KF160860 *Rhizophydium patellarium* voucher DAOM BR316
GQ995444 Rhizophydiales sp. AF011a
JN547302 Uncultured eukaryote clone V11-6
JQ689412 Uncultured Chytridiomycota clone Ay2007E5
AB971108 Uncultured Rhizophydiales clone Jp13Rp02E
GQ995446 Rhizophydiales sp. AF006
GQ995447 Rhizophydiales sp. AF005
HQ191408 Uncultured Chytridiomycota clone PA2009D12
HQ191367 Uncultured Chytridiomycota clone PA2009C21
HQ191359 Uncultured Chytridiomycota clone PA2009C19
HQ191385 Uncultured Chytridiomycota clone PA2009B12
HQ191301 Uncultured Chytridiomycota clone PA2009E23
AB971107 Uncultured Rhizophydiales clone Jp13Rp01E
HQ191360 Uncultured Chytridiomycota clone PA2009C20
HM135089 Uncultured fungus clone STFeb 269
EU162640 Uncultured Chytridiomycota clone PFD5SP2005
HQ191331 Uncultured Chytridiomycota clone PA2009A16
HQ191283 Uncultured Chytridiomycota clone PA2009E10
HQ191391 Uncultured Chytridiomycota clone PA2009B9c
EU162636 Uncultured Chytridiomycota clone PFB4SP2005
AF372719 Uncultured chytrid clone LEMD010
DQ536478 *Kappamyces laurelensis* isolate AFTOL-ID 690
NG 061053 *Kappamyces laurelensis* UACCC PL098
AF164263 *Alphamyces chaetifer* strain JEL39
GQ995432 Uncultured Chytridiomycota clone T6P2AeA07
GQ995431 Uncultured Chytridiomycota clone T5P1AeC04
GQ995429 Uncultured Chytridiomycota clone T5P1AeF01
GQ995430 Uncultured Chytridiomycota clone T5P1AeH04
KC561955 Uncultured Chytridiomycota isolate R11a 04
KC561958 Uncultured Chytridiomycota isolate R11a 10
KC561957 Uncultured Chytridiomycota isolate R11a 07
MH643793 Uncultured Rhizophydiales isolate SkChyt5
AH009034 *Rhizophydium* sp. UGA-F16
KC561952 Uncultured Chytridiomycota isolate E107 02D
KC561953 Uncultured Chytridiomycota isolate E107 05G
KC561954 Uncultured Chytridiomycota isolate E107 06G
KC561947 Uncultured Chytridiomycota isolate E109 08G
GQ995438 Uncultured Chytridiomycota clone T3P1AeE01
JN940949 *Rhizophydium* sp. *paterale*
DQ244004 Uncultured fungus clone PFF6AU2004
AY635821 *Rhizophydium* sp. JEL317 isolate AFTOL-ID 35
JN940945 *Aquamyces chlorogonii*
HM486997 Uncultured fungus clone GA043
HM487003 Uncultured fungus clone GA113
HM486999 Uncultured fungus clone GA077
HM487001 Uncultured fungus clone GA097
HM486996 Uncultured fungus clone GA001
HM487040 Uncultured fungus clone HA003
HM487042 Uncultured fungus clone HA042
AB971114 Uncultured Rhizophydiales clone Jp13Rp06E
AB971113 Uncultured Rhizophydiales clone Jp13Rp06S
AB971112 Uncultured Rhizophydiales clone Jp13Rp05E
JN940944 *Halomyces littoreus*
AB534324 Uncultured fungus clone A 3 27
GQ995448 Rhizophydiales sp. AF023
AB901696 Uncultured eukaryote clone AOox H 2012Dec 68
KT923284 Uncultured *Rhizophydium* clone Tea7
AH009035 *Rhizophydium macroporosum* JEL138
DQ244014 Uncultured fungus clone PFB11AU2004
AY601710 *Rhizophydium brooksianum* JEL136
Operculomyces laminatus strain JEL-223
DQ536492 *Rhizophydium* sp. JEL223 isolate AFTOL-ID 2007
DQ536485 *Rhizophydium* sp. JEL316 isolate AFTOL-ID 1535
LC274661 *Collimyces mutans*
GU568165 Uncultured soil fungus clone 8489
GU479968 Uncultured Rhizophydiaceae clone PR1 4E 45
FN690503 Uncultured fungus clone 5-E11
MT998435 *Ericiomyces syringoforeus* E4
DQ244013 Uncultured fungus clone PFD11AU2004
KP686527 Uncultured Rhizophydiales clone IN F03
HQ219436 Uncultured Chytridiomycota clone AY2009D13
HQ219429 Uncultured Chytridiomycota clone AY2009D12
HQ219378 Uncultured Chytridiomycota clone AY2009A4c
HQ219409 Uncultured Chytridiomycota clone AY2009B13
DQ103801 Uncultured marine eukaryote clone M2 18E09
DQ103819 Uncultured marine eukaryote clone M4 18F09
DQ103818 Uncultured marine eukaryote clone M1 18C05
DQ536488 *Rhizophydium* sp. MP8 isolate AFTOL-ID 1538
MH047189 Chytridiomycota sp.
AB971110 Uncultured Rhizophydiales clone Jp13Rp04S
AF164272 *Uebelmesseromyces harderi* strain JEL171
AY349048 *Uebelmesseromyces harderi* strain C29
KP686524 Uncultured Rhizophydiales clone IN E04
KP686535 Uncultured Rhizophydiales clone IN H03
KY555733 *Staurastromyces oculus* strain STAU-CHY2
KY350147 *Staurastromyces oculus* strain STAU-CHY3
KY555732 *Staurastromyces oculus* strain STAU-CHY1
DQ322622 *Boothiomyces macroporosum* isolate AFTOL-ID 689
NG017171 *Boothiomyces macroporosum* strain PL AUS 21
AH009032.2 *Rhizophydium sphaerotheca* strain JEL08
JN940947 *Rhizophydium sphaerotheca*
DQ536479 *Rhizophydium elyensis* isolate AFTOL-ID 693
MH023131 Uncultured *Rhizophydium* clone OTU783
AY349050 *Rhizophydium* sp. Bevill
AY349053 *Rhizophydium* sp. GSM3
AY349052 *Rhizophydium* sp. BR1
KJ464411 *Rhizophydium sphaerotheca*
DQ244005 Uncultured fungus clone PFB1AU2004
AB971115 Uncultured Rhizophydiales clone Jp13Rp07E
JQ689447 Uncultured Chytridiomycota clone Va2007BD10
AF164270.2 *Rhizophydium* sp. JEL151
AY635823 *Rhizophydium sphaerotheca* isolate AFTOL-ID 37
KF160859 *Gorgonomyces haynaldii* voucher DAOM BR100
HQ191313 Uncultured Chytridiomycota clone PA2009A3c
AY635824 *Entophlyctis* sp. JEL174 isolate AFTOL-ID 38
NG 065011 *Batrachochytrium salamandrivorans* CBS 135744
KC762294 *Batrachochytrium salamandrivorans* isolate AMFP13/1
AH009052 *Batrachochytrium dendrobatidis* strain JEL197
FJ799984 *Rhizophydium planktonicum* clone FMS34600
LC176286 *Rhizophydium planktonicum* strain AstB5
AH009061.2 *Rhizophydium* sp. UGA-F15
AH009051 *Homoloaphlyctis polyrhiza* strain JEL142

OUTGROUP

HQ901724 *Powellomyces hirtus* voucher Barr92
EF014367 *Entophlyctis confervae-glomeratae*
HQ901733 *Powellomyces hirtus* voucher JEL534
JQ014021 *Rhizophydium sphaerotheca* strain FSU 2509
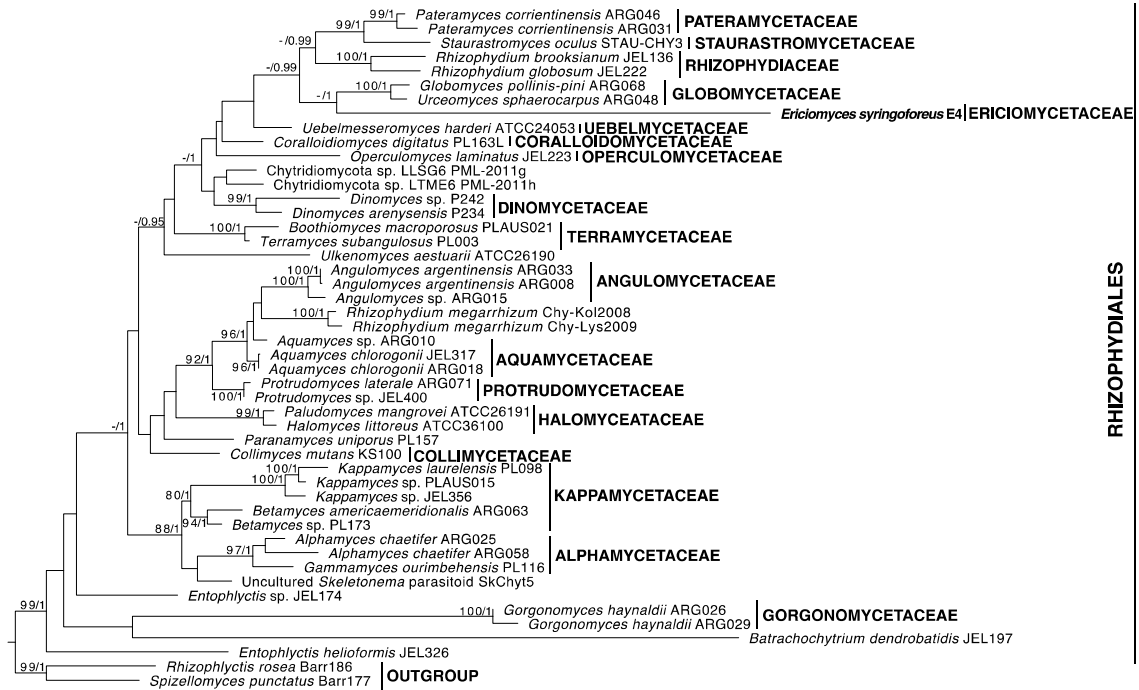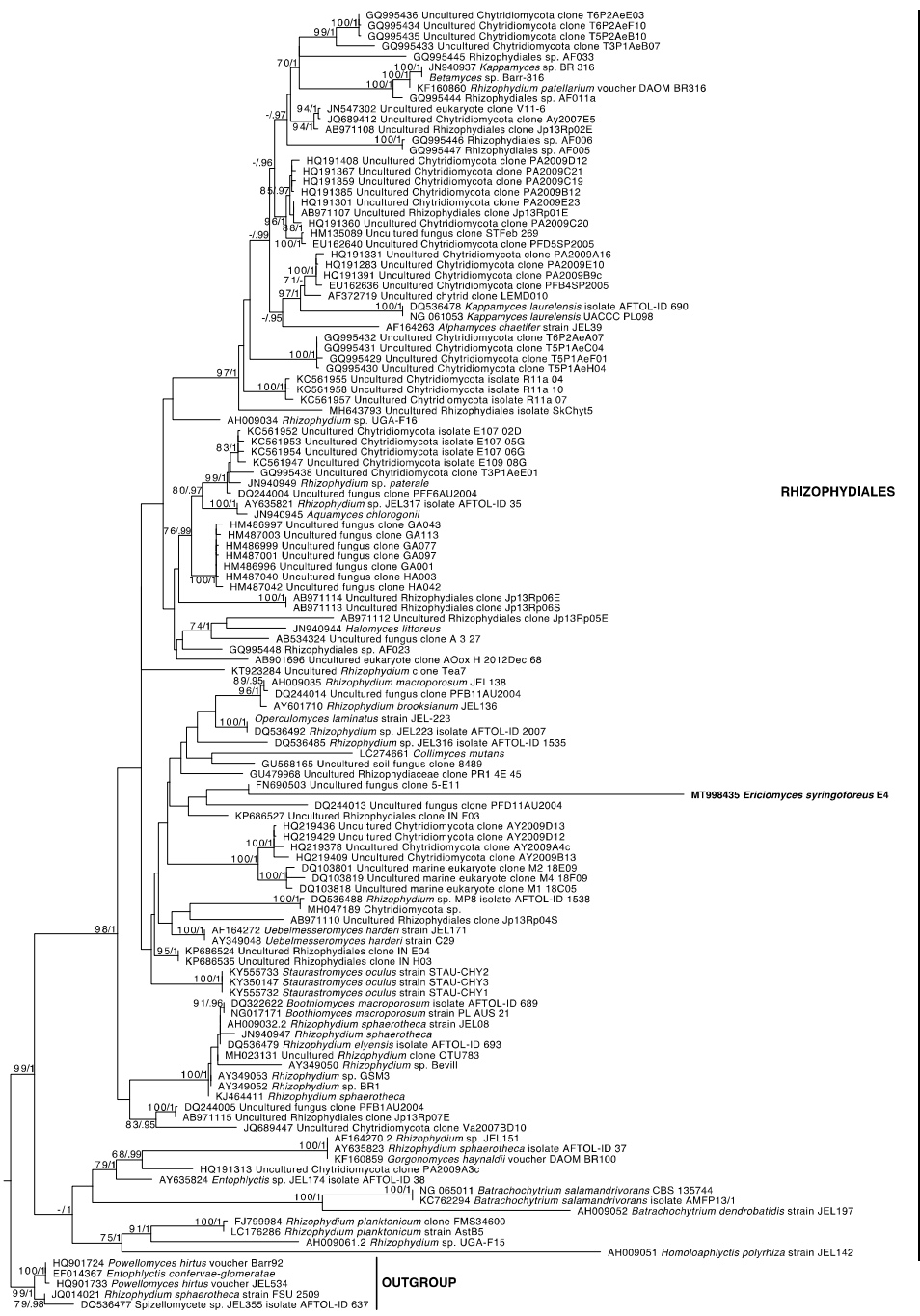DQ536477 Spizellomycete sp. JEL355 isolate AFTOL-ID 637

0.06

869

870 Supplementary Figure 3: Maximum likelihood phylogenetic tree of 18S rDNA sequences

871 representing the diversity of the Rhizophydiales. The sequence of *Ericiomyces syringoforeus* is

872 in bold. Statistical support of the nodes is presented by the bootstrap value (%) and the

873 Bayesian posterior probability. Only values >70% and >0.95 respectively are shown. When only

874 one of the values is below the threshold, it is indicated with a dashed line.

875

876